A Study of Higher-Order Mode Damping in an Adapted SRF Cavity Geometry

Charles Parker
Department of Electrical Engineering
Bucknell University
Lewisburg, PA 17837
(Dated: September 6, 2004)

The Laboratory for Elementary Particle Physics(LEPP) at Cornell University is proposing to expand their existing particle accelerator, CESR, by building a new linear accelerator that will be able to recover energy from the particle beam after it has been used. LEPP is currently prototyping portions of the proposed ERL. A copper model of an SRF injector cavity has been constructed. Modifications to the standard TESLA geometry have been made to help reduce and damp higher-order modes that are present in standard TESLA cavities. The copper model's ability to reduce and damp these modes has been measured, and the results are discussed herein.

I. INTRODUCTION

The idea of a particle accelerator that can recover energy from the unused beam was first thought of by M. Tigner in the 1960s. However, the successful demonstration of an energy recovery experiment with high beam current and energy at Thomas Jefferson National Accelerator Facility during the summer of 2003 has prompted the Laboratory for Elementary Particle Physics (LEPP) at Cornell University to design a prototype energy recovery linear accelerator (ERL)[2].

In order to maintain the stability of the beam, higher-order modes (HOMs) must be damped beyond what is required for conventional particle acceleration. LEPP is currently working on developing a prototype of the injector for a new ERL, which they are proposing to build at Cornell as an add-on to the existing particle accelerator, CESR.

A copper prototype of an SRF cavity to be used in this prototype has been designed and constructed. This cavity is similar to the standard TESLA SRF cavity, but deviates in a few important ways. One of the goals of these deviations is to reduce and damp HOMs that are present in the standard TESLA geometry.

II. CAVITY GEOMETRY

The geometry of the cavity we are experimenting with is similar to that of the TESLA cavity geometry. There are two primary differences: 1. twin input couplers, and 2. an enlarged beam tube on one end. This geometry was designed by V. Shemelin[3]

The purpose of the second input coupler is to increase the symmetry of the cavity's geometry. This will help reduce or eliminate the transverse kicks to the beam that are a result of the asymmetry of the TESLA cavities, which use only a single input coupler. Additionally, the presence of a second input coupler means that each input coupler only needs to be able to support half of the total forward power.

The enlarged beam tube acts like a high-pass filter. It was designed to have a cutoff frequency of 1658 MHz which is below the frequency of the this geometry's lowest dipole modes, but well above the frequency of the fundamental mode. This should allow any HOM with a frequency above 1658 MHz to propagate into the beam tube where it can be damped. Since the zero and pi modes are both well below this frequency, they should not propagate into the beam tube, and thus will not be damped with the HOMs.

The experiments discussed herein were performed on a copper prototype of this injector cavity.

Selected statistics for this modified geometry are shown in Figure 1.

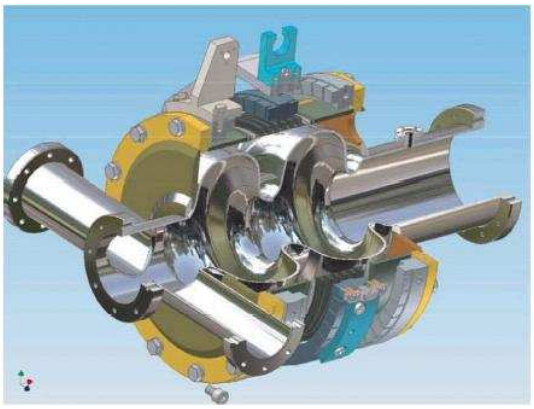

(a) Cavity cross section

Parameter	Value
Resonant frequency	1.300 GHz
Input coupler dia.	62 mm
Small end tube dia.	78 mm
Large end tube dia.	106 mm
Iris dia.	70 mm
Cell dia.	203 mm
Cell width	110 mm
Cavity length	536 mm
Material	Niobium
Operating temperature	2 K

(b) Cavity parameters

FIG. 1: Specifications of the new ERL injector cavity

III. EXPERIMENTATION

With these experiments we would like to determine which HOMs are present in the cavity, the type of each mode that is present, and how strongly those modes are damped by propagation through the beam tubes.

Our primary tools for conducting these experiments are LabView, and an HP 8753C Network Analyzer with an 85047A S-Parameter Test Set.

Two scenarios exists for taking measurements: 1. metal caps on the ends of the beam tubes, 2. removing these caps and allowing the tubes to be open. Scenario 1 reflects more accurately the way our theoretical model was constructed while scenario 2 more accurately reflects the environment the cavity will be in when installed in the injector prototype. In order to validate our model and also make predictions about how the cavity will respond when in the injector prototype, we have taken data in both scenarios.

All experiments were conducted at room temperature.

Our first experiment is a measurement of the frequency response of the cavity. From this measurement we can locate resonant frequencies of the cavity. To do this we used the

network analyzer to measure the loss of RF power in transmission through the cavity. The network analyzer communicated with a LabView program which recorded data every 1.3 kHz from 1 to 6 GHz. By visually examining a plot of this data resonant frequencies can be identified.

After identifying the resonant frequencies of the cavity we can begin to measure the axis field and the Q of each resonance.

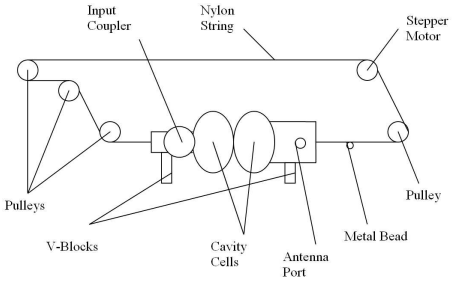

FIG. 2: Experimental Setup

FIG. 3: Copper model of the modified ERL injector cavity geometry

To measure the field along the axis of the cavity we can use a bead pull experiment. Theory presented by L. Maier and J. Slater in 1952 [1] tells us that the electric and magnetic field strength at a point in the cavity determines the shift in resonant frequency of the cavity when it is perturbed at that point. Using this theory, we can perturb the cavity using a small conductor placed at the point where we would like to measure the field. The shift in resonant frequency is a quantity that can be measured using a network analyzer. We can then calculate the field at the perturbed point.

Our experimental setup uses pulleys to hold a nylon string along the cavity's axis. This string is taught so that there is virtually no deviation from the cavity's axis. On this string is the metal bead that perturbs the cavity. The bead is moved along the axis of the cavity while the resonance of the cavity is monitored by the network analyzer. Christopher Cooper wrote the LabView program to control this experiment. The LabView program collects data from the network analyzer and moves the bead using a stepper motor. A diagram of the experimental setup can be seen in Figure 2.

The last measurement we would like to make is the Q of each resonance. The network analyzer has a built in function to measure this parameter. We used a LabView program to take a number of these measurements for each mode. We took the mean of these measurements as our result.

It is also possible to calculate the Q of a mode from the data taken in the initial frequency scan. Matthias Liepe has prepared a Matlab program to do this. This program fits a polynomial to the resonance spikes and uses these fits to calculate Qs, reducing the effect of noise in the measurement. This approach can also be better then measuring the Qs directly because the data it operates on is taken without moving the antennas. The position of the antennas in the cavity can have a significant effect on the measured Q of many modes.

IV. RESULTS

The axis field profiles serve three purposes. First, profiles matching the profiles our model predicted validates our model. Second, profiles allow us to keep track of modes when we

change the experimental configuration. This is necessary because when a factor is changed even slightly (for example, placing one antenna slightly farther into the antenna port) the frequencies of the modes will shift. Third, the profiles allow us to determine what kind of mode we are looking at. If we find a large resonance spike and measure very little field on the axis of the cavity, it is likely that the mode we are looking at is a quadrupole mode. If we do measure a significant amount of field on axis, then we are more likely looking at a monopole or dipole mode.

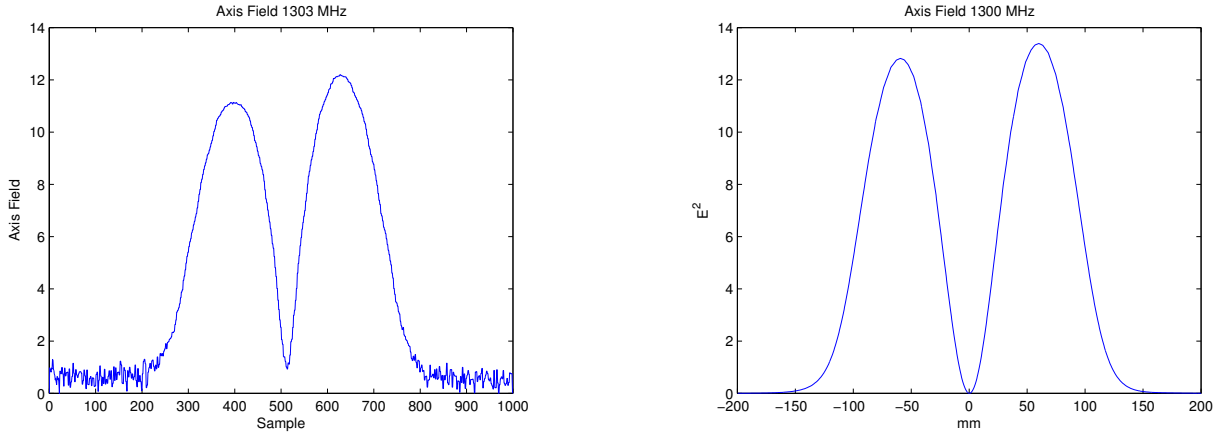

(a) Measured profile

(b) Theoretical profile

FIG. 4: Cavity axis field profiles of the fundamental mode

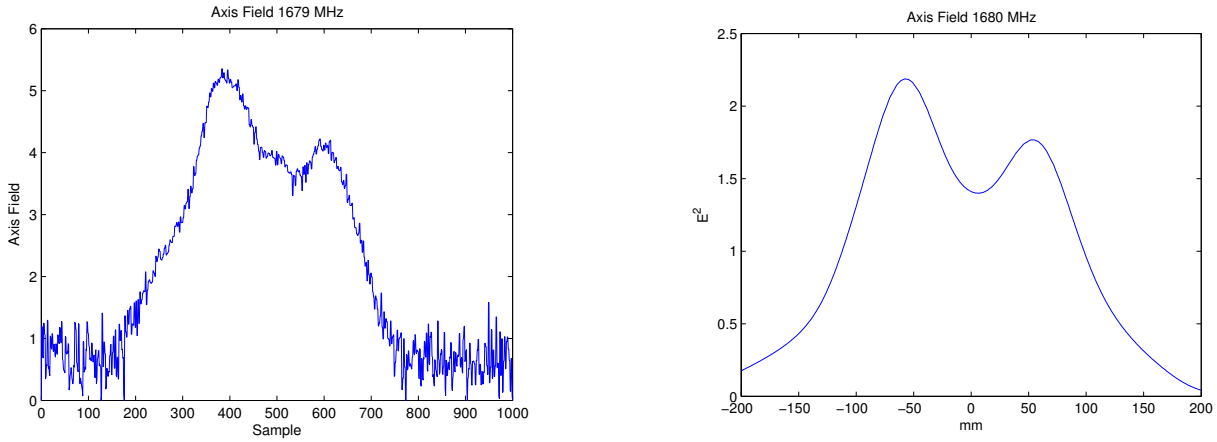

(a) Measured profile

(b) Theoretical profile

FIG. 5: Cavity axis field profiles of mode at 1.680 GHz

Figures 4 and 5 show examples of field profiles that were measured matched up with predicted field profiles. Generally, the measured field profiles matched up well with our predictions.

In figure 4 the magnitudes of the humps are not equal. This is true for both the prediction and the measurement. In the measurement this is the result of the cells being slightly out of tune. However, the humps are easily within 10% of each other. This indicates that the dissonance between the two cells is very small. This consistency also tells us that the fields in the cavity are very homogeneous.

Another discrepancy arose in the frequency of physical cavity when compared with the models prediction. The model predicted that the pi-mode resonance would occur at 1.2998 GHz. We measured it to be at 1.303 GHz. This is likely due to small flaws from the manufacturing process.

The graphs in figure 6 give a general overview of our results. When the end caps are removed many of the resonance spikes completely disappear, and the rest are significantly reduced in size. This means that many HOMs are propagating through the larger beam tube where they are being damped, which is what we predicted would happen.

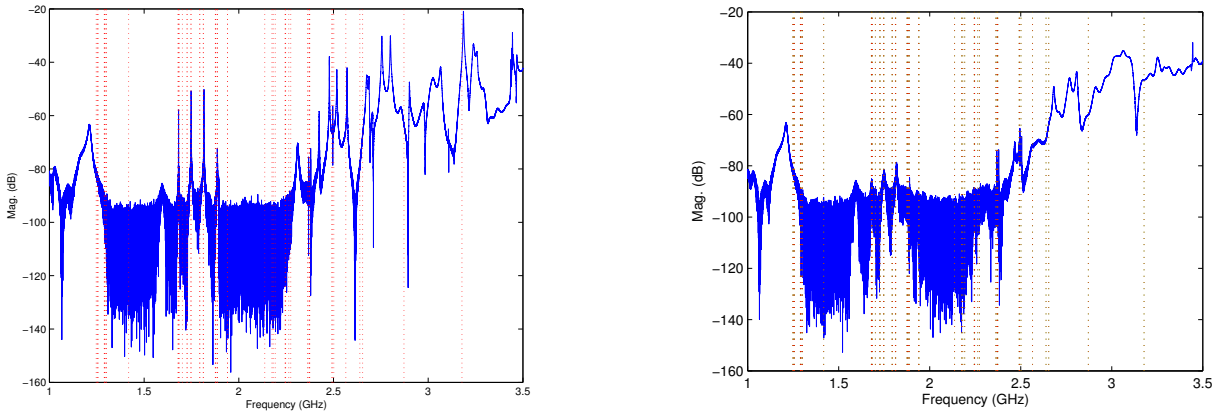

(a) Frequency response with end caps

(b) Frequency response with out end caps

FIG. 6: Frequency response of the copper prototype ERL injector cavity

The vertical lines in figure 6 denoted frequencies at which our model predicted modes would be present. There are not spikes at all of these locations because this set of data was taken from only one antenna position. Because some modes have no field at many places in the cavity, an antenna placed at one of these locations will not couple to that mode. Consequently, to see all the modes the antenna position must be shifted.

Table I shows the frequencies of the predicted modes, and the Q measurements with and with out end caps. This table only includes dipole modes up to 2.2 GHz and the lowest quadrupole mode.

Figure 7 shows all the measured Qs below 3.5 GHz. When the end caps are removed, the average value of the Qs drops considerably, and many modes have Qs too low to be

measured. In figure 7(a) you can see the Q of one spike from each of the four lowest dipoles clustered between 1.5 and 2 GHz. Another feature that stands out is three Qs from the lowest quadrupole, and one from the second quadrupole. Comparing figure 7(a) with figure 7(b) we can see that the lower dipoles are damped significantly when allowed to propagate through the end tubes, while the lowest quadrupole remains present. This agrees with the predictions of our model that require modes having having significant field in and being above the cutoff frequency of the end pipes (1658 MHz) to be damped.

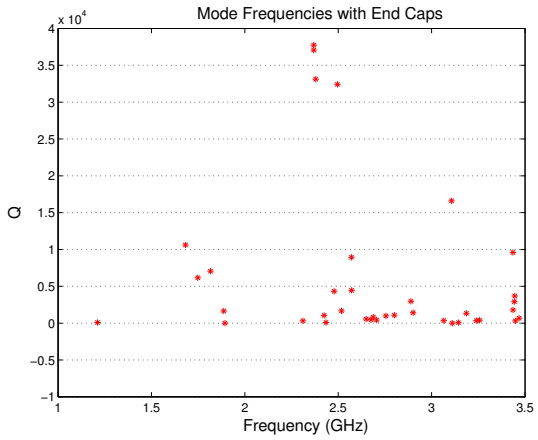

(a) Measurements with end caps

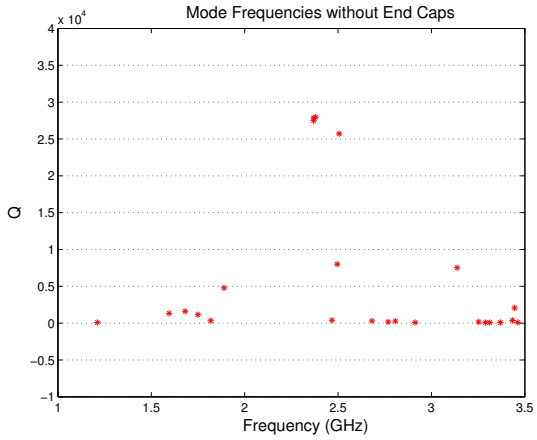

(b) Measurements without end caps

FIG. 7: Mode frequencies and associated Qs

Mode type	f_{calc} (GHz)	f_{meas} (GHz)	Δf (MHz)	Q with end caps	Q without end caps	Q_{proper}
TM_{010}	1.29033	1.29376	+3.49634	3.47e4	2.84e4	$> 10^5$
TM_{010}	1.29936	1.30300	+3.69800	3.11e4	2.73e4	$> 10^5$
Dipole 1-1	1.67992	1.67867	-1.24445	1.61e4	not found	N/A
Dipole 1-2	1.68348	1.68200	-1.48100	1.06e4	1.60e3	1.88e3
Dipole 2-1	1.72700	1.73600	+9.00460	3.49e3	not found	N/A
Dipole 2-2	1.74863	1.74810	-1.29000	6.16e3	1.15e3	1.41e3
Dipole 3-1	1.79387	1.80410	+10.2421	1.73e4	not found	N/A
Dipole 3-2	1.81342	1.81800	+5.67100	7.06e3	3.26e2	3.42e2
Dipole 4-1	1.87647	1.86800	+8.46528	2.04e3	not found	N/A
Dipole 4-2	1.87661	1.87800	-1.40301	could not measure	not found	N/A
Quadrupole 1-1	2.36432	2.36870	-4.37514	3.77e4	2.75e4	$> 10^5$
Quadrupole 1-2	2.36468	2.36890	-4.27843	3.71e4	2.79e4	$> 10^5$
Quadrupole 1-3*	2.37233	2.37930	-6.96899	3.31e4	2.80e4	$> 10^5$
Quadrupole 1-4*	2.37375	2.37930	-5.55459	3.31e4	2.80e4	$> 10^5$

TABLE I: Resonance frequencies and Q measurements

* only one of these modes was found. It is impossible to determine if the found mode is quadrupole 1-3 or quadrupole 1-4.

Our model predicted the frequencies of the modes quite well, as can be seen in column 4 of table I. It is interesting to note that the lower mode of all four dipoles could not be found without end caps. Also, the lower mode of dipoles 2, 3 and 4 all have a much larger discrepancy in predicted and measured frequency. Upon inspection of the model, the lower mode of all four dipoles has a significant amount of field in the plane of the input coupler while the higher modes have more field in the plane perpendicular to the plane of the input couplers.

It is easy to question the usefulness of our Q measurements since the cavities to be used in the ERL will be superconducting and made of Niobium. Warm cavities have significantly more losses because the cavity walls are not superconducting and thus quite lossy. It is, however, possible to calculate the losses due to propagation and due to wall loss by comparing the Qs with and without end caps on the cavity. This is the quantity Q_{proper} in table I. It's given by:

$$\frac{1}{Q_{proper}} = \frac{1}{Q_{noendcaps}} - \frac{1}{Q_{withendcaps}} \tag{1}$$

V. CONCLUSIONS

While the copper prototype performed as we expected, allowing HOMs to propagate out of the cavity to be damped, the tolerances on the frequencies of these modes were large due to manufacturing error.

Additional experiments will need to be conducted with a more precisely made cavity, and under operating conditions (i.e. a niobium cavity at 2 K).

VI. ACKNOWLEDGMENTS

I would like to acknowledge Dr. Matthias Liepe for his help and guidance on this project in addition to conceiving it. I would also like to thank Rich Galik for coordinating and supporting the REU program at Cornell. Finally, I'd like to thank the National Science Foundation for supporting this research under grant PHY-0243687 and research co-operative agreement PHY-9809799.

---

[1] Maier, L. and J. Slater."Field Strength Measurements in Resonant Cavities." Journal of Applied Physics Vol. 23, No. 1 (1952).

[2] Study for a proposed Phase I ERL Synchrotron Light Source at Cornell University, ed. by S. Gruner and M. Tigner, CHESS Tech. Memo 01-003, JLAB-ACT-01-04 (July 2001).

[3] V. Shemelin et al., Proceedings of the 2003 Particle Accelerator Conference, Oregon, May 2003, paper WPAB012 (2003).